Impact of the parton distribution function uncertainties on the measurement of the W boson mass at the Tevatron and the LHC

G. Bozzi,* J. Rojo,† and A. Vicini‡

(Received 14 April 2011; published 20 June 2011)

We study at a quantitative level the impact of the uncertainties on the value of the W boson mass measured at hadron colliders due to: i) the proton parton distribution functions (PDFs), ii) the value of the strong coupling constant α_s and iii) the value of the charm mass used in the PDF determination. The value of the W boson mass is extracted, by means of a template fit technique, from the lepton-pair transverse mass distribution measured in the charged current Drell-Yan process. We study the determination of m_W at the Tevatron and at the LHC with 7 and 14 TeV of center-of-mass energy in a realistic experimental setup. The analysis has been done at the Born level using the event generator HORACE and at NLO-QCD using the event generators DYNNLO and RESBOS. We consider the three global PDF sets, CTEQ6.6, MSTW2008, and NNPDF2.1. We estimate that the total PDF uncertainty on m_W is below 10 MeV both at the Tevatron and at the LHC for all energies and final states. We conclude that PDF uncertainties do not challenge a measurement of the W boson mass at the level of 10 MeV accuracy.

DOI: 10.1103/PhysRevD.83.113008 PACS numbers: 14.70.Fm

I. INTRODUCTION

The measurement of the W boson mass represents a very important test of the standard model and of its extensions, like e.g. the minimal supersymmetric standard model, and provides indirect bounds on the mass of the Higgs boson [1–3]. This measurement has reached a very high level of accuracy: the current world average is $m_W = 80.398 \pm 0.023$ GeV [4] and the best single experiment measurements have been obtained by D0 [5] and CDF [6,7] at the Fermilab Tevatron with $m_W = 80.401 \pm 0.043$ GeV and $m_W = 80.413 \pm 0.048$ GeV respectively. The prospects for the combined measurements at the end of the Tevatron run, with 4 fb^{-1} of total collected luminosity, are of a final error of roughly 15 MeV [8]. The prospects for the measurement at the CERN LHC are at the level of 15 MeV, or even 10 MeV [9,10]. At this level of accuracy, it becomes necessary to quantify in detail the various sources of theoretical uncertainties that contribute to the final systematic error.

The mass of the W boson is measured at hadron colliders in the charged current Drell-Yan (DY) process by studying the charged lepton transverse momentum p_t^l distribution, the missing transverse momentum p_t^ν distribution, or the lepton pair transverse mass distribution, defined as

$$M_\perp^W = \sqrt{2p_t^l p_t^\nu (1 - \cos(\phi^l - \phi^\nu))}, \tag{1}$$

where the neutrino four-momentum p_t^ν and angle ϕ^ν are inferred from the transverse momentum imbalance in the event. The mass of the W boson is obtained by fitting the experimental distributions with the corresponding theoretical predictions, where m_W is kept as a free parameter.

A measurement of m_W at the 10 MeV level is not only a very ambitious goal from the experimental side, but it is also very challenging from the theoretical point of view due to the careful modelling of the production mechanism that is required. We can illustrate these difficulties with the following example. It is known that the result of a fit of m_W to a given theory template is very sensitive to the shape of the distributions. In Fig. 1, we consider two transverse mass distributions at the Born level obtained with two values of m_W which differ by 10 MeV. If one takes the ratio bin by bin of the histograms, one sees that a small shift of 10 MeV in m_W induces a non trivial distortion of the shape at the permille level. Therefore, if we aim at measuring m_W at the 10–20 MeV level, we should, from the theoretical side, have the control on all the perturbative and nonperturbative corrections which can change the shape of the relevant kinematic distributions at this level of precision.

On the other hand, the total integrated cross section is not significantly affected by changing m_W. As shown in Table I, a shift by 10 MeV of m_W yields a change of the cross section at the 0.04% level. Thus, it is important to disentangle the normalization effects, which are very weakly related to the precise value of m_W, from the effects that modify instead the shape of the distributions, which have a larger impact on the measurement of m_W.

The Drell-Yan cross section is given by the convolution of the parton distribution functions (PDFs) of the two incoming hadrons with the partonic cross section. The crucial role of QCD corrections to the partonic processes has been widely discussed in the literature [11,12]. The very important role of the $\mathcal{O}(\alpha)$ EW corrections in the precision study of the charged current DY process is also well known (for a complete list of references, see [13]). It is the aim of the present paper to study three different

*Email: Giuseppe.Bozzi@mi.infn.it
†Juan.Rojo@mi.infn.it
‡Alessandro.Vicini@mi.infn.it

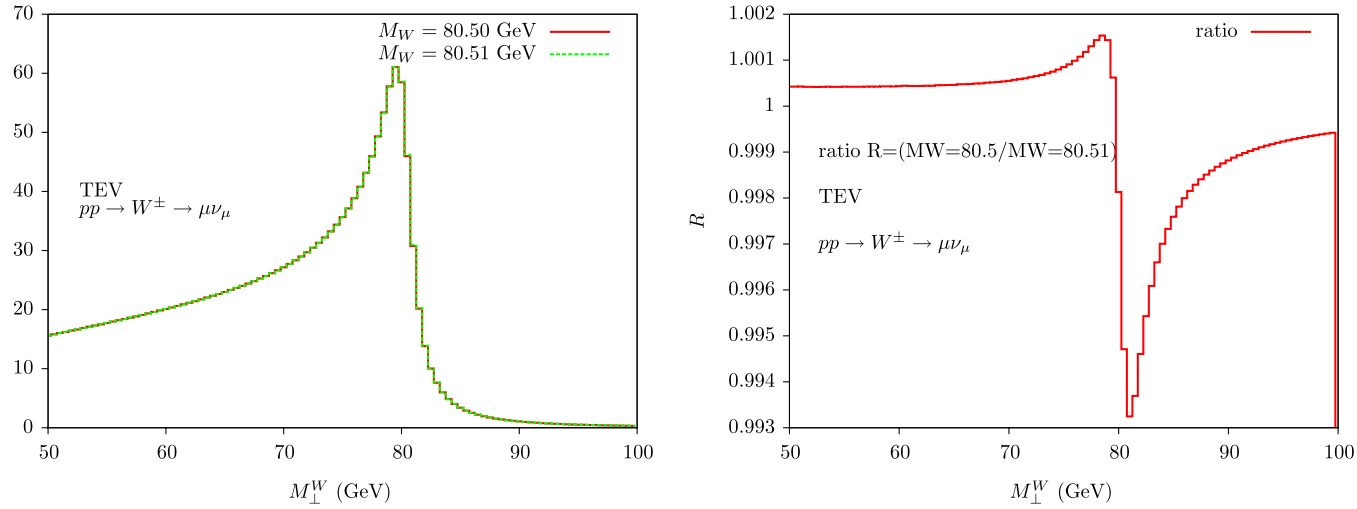

FIG. 1 (color online). Left plot: the transverse mass distributions at the Tevatron at Born level obtained with two values of m_W which differ by 10 MeV. Right plot: the bin by bin ratio of these two distributions.

sources of uncertainty related to the PDFs and their impact on the measurement of m_W:

(1) the PDFs are affected by uncertainties due to the error of the experimental data from which they are extracted, as well as by theoretical uncertainties like the nonperturbative functional form parametrization. These uncertainties affect the prediction of the DY observables and, in turn, the extraction of the value of m_W. Moreover in some cases the central values obtained from different PDF sets differ more than the nominal PDF uncertainties: we need to account for this by considering more than one PDF set;

(2) the NLO-QCD corrections sizably modify the Born-level lepton transverse momentum distribution and, more moderately, also the transverse mass distribution. The precise effect of these corrections depends on the value of the strong coupling constant, which is ultimately correlated with the PDFs and with their evolution. Therefore, the precise value of α_s should also be taken into account in a precision determination of m_W;

(3) the PDFs depend on the value of the heavy quark masses m_c and m_b due to two different reasons: the first one is the fact that $\mathcal{O}(m_c^2/Q^2)$ terms have a non-negligible impact on PDF fits, and the second that heavy quark PDFs are obtained by assuming them to vanish at threshold, and then to be generated by perturbative evolution. For these reasons, the value of the m_c used in the PDF determination has an impact on the kinematic distributions from which m_W is extracted, and thus must be accounted for. The value of m_b on the other hand does not affect W production due to the smallness of b-initiated contributions.

Uncertainties related to PDFs are known to be an important component of the total systematic error in the determination of m_W at hadron colliders. In the most recent CDF and D0 measurements, PDF uncertainties are estimated to be between 10 and 13 MeV [4]. Reference [10] estimates PDF errors in m_W prior to LHC data to be $\sim$25 MeV, decreasing at the few MeV level once the constraints from LHC processes are taken into account. On the other hand, there are claims [14] that with the current knowledge of PDFs a determination of m_W with a precision $\Delta m_W \leq 10$ MeV is far from being possible. In this paper, we want to revisit the impact of PDFs and related uncertainties on the determination of m_W at the Tevatron and the LHC, considering the most updated global PDF sets and related theoretical uncertainties, like the values of α_s and m_c.

The paper is organized as follows. In Sec. II, we present the general strategy that we will follow to estimate the shifts of the measured value of m_W induced by PDF uncertainties. In Sec. III, we present the numerical results of our analysis for the transverse mass distribution, and in

TABLE I. Cross sections within acceptance cuts, at Born level, as a function of m_W. We also show the percentage difference between pairs of cross sections that differ by 10 MeV.

m_W (GeV)	80.368	80.378	80.388	80.398	80.408	80.418
$\sigma_{\rm tot}(m_W)$ (pb)	368.72	368.87	369.03	369.17	369.32	369.46
$(\sigma_{\rm tot}^{i+1} - \sigma_{\rm tot}^{i})/\sigma_{\rm tot}^{i}$		0.04%	0.04%	0.04%	0.04%	0.04%

Sec. IV the results for the PDF impact on the determination of m_W. InSec. V, we explore the improvements on PDF uncertainties for the determination of the W mass provided by LHC data, and in Sec. VI we draw our conclusions.

II. THE DETERMINATION OF m_W: GENERAL STRATEGY

In this section, we present the general strategy that we adopt to estimate the impact of PDF uncertainties in the determination of m_W at hadron colliders. First of all, we introduce the fitting procedure and its validation. Then we discuss the event generators and settings adopted to compute the theoretical distributions. Finally, we discuss the PDF sets that are considered in this study together with related sources of theoretical uncertainty.

A. The fitting procedure and its validation

We consider in the present study differential distributions in charged current Drell-Yan production generated with different PDF sets and we treat them as samples of pseudodata. The Monte Carlo error on each bin is taken in the statistical analysis as the error affecting the pseudodata. The pseudodata are generated with a given common nominal value of m_W called m_W^0, which is taken to be $m_W^0 = 80.398$ GeV, the current world average.

The general fitting strategy is summarized in Fig. 2. First of all, we generate the templates for a given fixed PDF set, in this case the central set of CTEQ6.6, and for different values of m_W, with very high statistics, 1B events at Born level. Then for each member of the PDF sets considered, including the error PDF sets, we generate pseudodata with fixed $m_W^0 = 80.398$ GeV using exactly the same event generator as for the templates, with lower statistics, 100 M events at Born level. Then we compute the χ^2 between the pseudodata and each of the templates: the template with best χ^2 provides the information on which is the shift in m_W induced by this particular PDF set. As expected for consistency when pseudodata is generated with the central CTEQ6.6 set, we get $\chi^2 \sim 1$ for the selected template with $m_W = m_W^0$.

The templates have been computed for 100 (at Born level) and 20 (at the NLO-QCD level) different values of the W mass. The range for these templates has been taken to be 80.398 ± 0.050 MeV at Born level and 80.398 ± 0.036 at NLO-QCD. We compare each template with the pseudodata and compute the reduced χ^2 function, defined as

$$\chi^2_j = \frac{1}{N_{\rm bins}} \sum_{i=1}^{N_{\rm bins}} \frac{(\mathcal{O}_i^j - \mathcal{O}_i^{\rm data})^2}{(\sigma_i^{\rm data})^2} \qquad j = 1, \ldots, N_{\rm templates} \tag{2}$$

where $\mathcal{O}_i$ is the value of the i-th bin of the distribution $\mathcal{O}$ (e.g., the W transverse mass) and the superscript refers to the pseudodata or to the j-th template. The value of m_W used in the template which minimizes χ^2_j is considered as the preferred value of m_W and the difference $\Delta m_W = m_W - m_W^0$, is the shift induced by the PDF set chosen for that set of pseudodata. A similar approach has been used in [10,15,16].

The fitting procedure has been validated by using samples of pseudodata that have been produced with the same inputs and the same event generator of the templates but with different statistics. In this case the function χ^2 defined in Eq. (2) can be used to make a χ^2-test. When

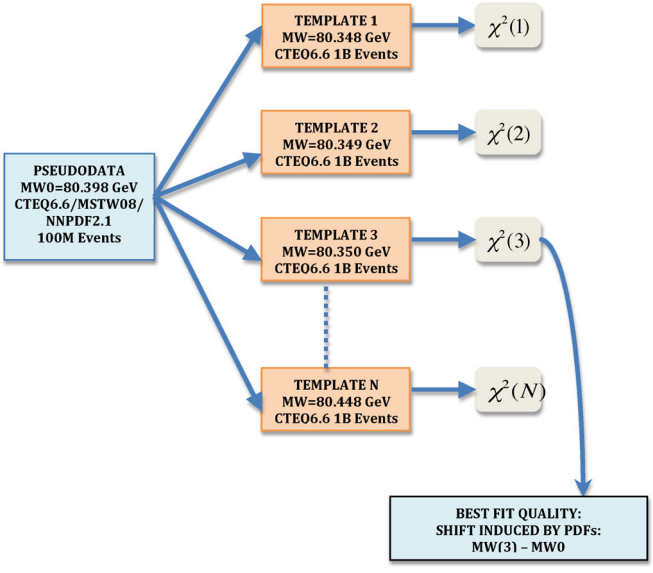

FIG. 2 (color online). Flowchart that summarizes the procedure used to determine the shift in m_W induced by any given PDF set. More details are provided in the text.

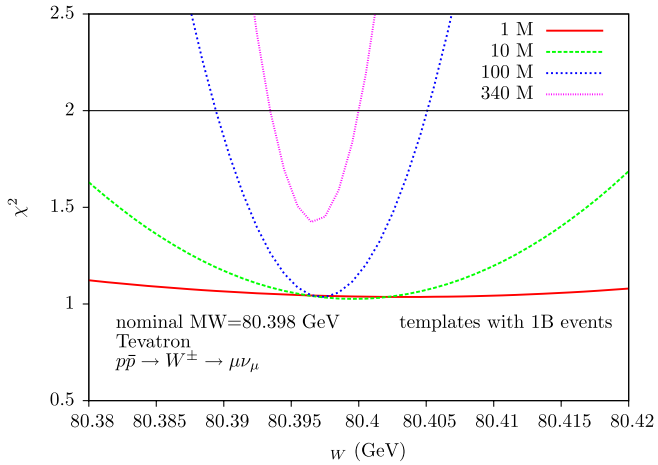

FIG. 3 (color online). χ^2 distributions obtained fitting Born level pseudodata with Born level templates for the same fixed PDF set at the Tevatron kinematics. The different curves correspond to different pseudodata samples each with different statistics. The $\Delta\chi^2 = 1$ rule indicates the resolution, at 68% C.L., on the W mass.

fitting pseudodata obtained with a given event generator, the nominal value of m_W used in the generation of the data is rediscovered as preferred value within an interval determined by the condition $\Delta\chi^2 = 1$, which can be interpreted as a 68% C.L. interval. This interval shrinks as the number of events considered increases and correspondingly their statistical fluctuations are damped, as shown in Fig. 3. In this example, the templates have been generated with 1B events while the pseudodata has been generated with increasing statistics from 1 M to 340 M events. We also checked that, fitting 1000 independent samples of Born level pseudodata, the corresponding minima follow the χ^2 distribution, as expected.

When the statistics of the pseudodata become close to those of the templates, the χ^2 can deteriorate since it becomes sensitive to the statistical fluctuations of the latter, not accounted for in Eq. (2). This imposes a practical limit on how accurate the pseudodata can be. This effect can be seen in Fig. 3 for the case of pseudodata generated with 340 M events. We find that a good compromise between resolution and stability with respect to fluctuation is provided by using templates of 1B events with pseudodata generated with 100 M events.

B. Event generation

Let us discuss now how the theoretical predictions of the DY kinematic distributions have been generated. We have studied the production process $p\bar{p} \to \mu^+ + X$ at the Tevatron Run II ($\sqrt{s} = 1.96$ TeV). We also consider the two processes $pp \to \mu^+ + X$ and $pp \to \mu^- + X$ at the LHC for $\sqrt{s} = 7$ TeV and $\sqrt{s} = 14$ TeV center–of–mass energies. In the absence of QED effects, not considered here, our results will be identical to those obtained with electrons instead of muons. The numerical results have been obtained using the following values for the input parameters:

$G_\mu = 1.16637 \times 10^{-5}$ GeV^{-2}	$m_W = 80.398$ GeV	$m_Z = 91.1876$ GeV
$\Gamma_W = 2.141$ GeV	$\sin^2\theta_W = 1 - m_W^2/m_Z^2$	$m_H = 120$ GeV
$V_{cd} = 0.222$	$V_{cs} = 0.975$	$V_{cb} = 0$
$V_{ud} = 0.975$	$V_{us} = 0.222$	$V_{ub} = 0$
$V_{td} = 0$	$V_{ts} = 0$	$V_{tb} = 1$

The charm quark in the partonic cross section is treated as a massless particle, while the bottom quark does not contribute because of the vanishing top density in the proton.

In the generation of Drell-Yan charged current events, we used the selection criteria summarized in Table II.

TABLE II. Selection criteria for $W^\pm \to l^\pm \nu$ events for the Tevatron and the LHC.

Tevatron	LHC
$p_\perp^\mu \geq 25$ GeV	$p_\perp^\mu \geq 25$ GeV
$\not{E}_T \geq 25$ GeV	$\not{E}_T \geq 25$ GeV
$\lvert\eta_\mu\rvert < 1.0$	$\lvert\eta_\mu\rvert < 2.5$

These kinematic cuts are similar to those used in the corresponding experimental analysis. Note that the main difference between the Tevatron and LHC cuts is a wider acceptance for the rapidity of the leptons in the latter case. The W transverse mass distribution has been studied in the interval 50 GeV $\leq M_\perp^W \leq$ 100 GeV, with a bin size of 0.5 GeV, since the Jacobian peak region is the most sensitive for the determination of m_W. All the following analyses are performed with bare leptons both in the pseudodata and in the templates.

The pseudodata and the templates have been generated using the following event generators: at Born level with HORACE [17], at NLO-QCD with DYNNLO [18] and at NLO + NNLL-QCD with RESBOS [19]. These generators allow to compute the distributions of the final state leptons in the DY processes at various perturbative orders. For example, RESBOS includes, on top of the NLO-QCD corrections, part of the NNLO-QCD terms matched with the resummation of the large $\log(\frac{p_\perp^W}{m_W})$ at leading logarithmic and next-to-leading logarithmic accuracy, and has been widely used at the Tevatron.

Our final results for the determination of m_W will be those obtained at NLO-QCD with DYNNLO, although, as we will show below, the qualitative results are already very similar at Born level.

C. PDF uncertainties

The proton PDF sets considered in this study are the three global sets that include all the relevant hard scattering data. In particular, we will use the NLO-QCD CTEQ6.6 [20], MSTW2008 [21], and NNPDF2.1 [22] PDF sets. Each collaboration provides a prescription to estimate the PDF uncertainties:, in particular, we recall the formula for the symmetric error in the Hessian approach (CTEQ,MSTW)

$$\Delta X = \frac{1}{2}\sqrt{\sum_{i=1}^{N}[X_i^+ - X_i^-]^2} \tag{3}$$

and the average over the ensemble of PDF replicas (NNPDF)

$$\langle \mathcal{F}[\{q\}]\rangle = \frac{1}{N_{\rm rep}}\sum_{k=1}^{N_{\rm rep}} \mathcal{F}[\{q^{(k)}\}]$$

$$\sigma_{\mathcal{F}} = \left(\frac{1}{N_{\rm rep}-1}\sum_{k=1}^{N_{\rm rep}}(\mathcal{F}[\{q^{(k)}\}] - \langle \mathcal{F}[\{q\}]\rangle)^2\right)^{1/2}.$$

We refer to the original publications as well as to the recent reviews [23–25] for more details. Let us recall that the use of the three global PDF sets is the basis of the current PDF4LHC recommendation [26] for the use of PDFs in the analysis of LHC data.

On top of the PDF uncertainties that arise from the experimental uncertainties of the data used in their determination, there are other sources of theoretical

uncertainties closely related to PDFs. In the first place, PDFs are correlated with the value of the strong coupling constant $\alpha_s(m_Z)$ used in the PDF determination, especially the gluon PDF. Again, all three groups provide prescriptions on how to combine the PDF and strong coupling uncertainties in a consistent way. A summary of the prescriptions recommended by each group can be found in the PDF4LHC working group interim report [25] (see also Ref. [27]). A practical guide on the way to efficiently implement the recommendations by the different groups can be found in Ref. [28]. While the impact of variations on the value of $\alpha_s(M_Z)$ are known to be small for vector boson production,[1] they may need to be taken into account at the level of precision required for the determination of m_W.

On top of the value of the strong coupling, PDFs depend as well on the value of the heavy quark masses m_c and m_b due to two different reasons. The first one is the fact that even though most LHC perturbative computation are done up to power-suppressed terms, terms of $\mathcal{O}(m_h^2/Q^2)$ do still have a non-negligible impact on PDF fits, especially to the HERA collider data. Power-suppressed terms are accounted for in the various General–Mass VFN schemes used in modern PDF sets [30–32], and the choice of m_c affects the GM-VFN predictions and thus the fitted PDFs. Different GM-VFN schemes have been compared in the Les Houches heavy quark benchmark study [33], elucidating their differences and similarities.

The second reason has simply to do with the fact that heavy quark PDFs are obtained by assuming them to vanish at threshold, and then to be generated by perturbative evolution. But changing the mass also changes the position of the threshold, and thus the heavy quark PDFs (and their contribution to the cross section) depend on the value of m_h. For example, for W production, the initial state with one charm and one strange quarks occurs at the Born level approximately in the 7% of the cases at the Tevatron, in the 16% at LHC 7 TeV for W^+ production and in the 25% for W^- production, in the 24% at LHC 14 TeV for W^+ production and in the 32% for W^- production.

For these reasons, the precise value of the m_c has an impact on the kinematic distributions from which m_W is extracted and must be accounted for, especially since charm mass variations are known to induce sizeable effects for W production at colliders [22,34].

III. PDF UNCERTAINTIES FOR THE TRANSVERSE MASS DISTRIBUTION

Now that the setup of the analysis has been presented, we consider how PDFs and related uncertainties affect the lepton pair kinematic distributions, in particular, the transverse mass distribution, and in the next section we will consider their impact on the determination of m_W. As discussed in Sec. II, only those sources of uncertainties that induce distortions on the shape of the distribution (rather than on its normalization) will have an impact for the extraction of m_W.

The transverse mass distribution has the advantage, with respect to the lepton p_T distribution, that QCD-NLO corrections are rather moderate and, in particular, have a small effect on the shape of the distribution. Experimental issues in its measurement like the systematic uncertainties due to the neutrino p_T reconstruction are not addressed here.

In the following, we will consider two related distributions: the transverse mass distribution,

$$\mathcal{O}(M_\perp^W) \equiv \frac{d\sigma}{dM_\perp^W}(M_\perp^W),$$
$$M_\perp^W = \sqrt{2p_t^l p_t^\nu (1-\cos(\phi^l-\phi^\nu))}, \qquad (4)$$

and the same distribution but normalized to the integrated cross section in the region used for the m_W fit,

$$\tilde{\mathcal{O}}(M_\perp^W) \equiv \frac{1}{\sigma^{\rm fit}}\frac{d\sigma}{dM_\perp^W}(M_\perp^W),$$
$$\sigma^{\rm fit} \equiv \int_{M_\perp^{W,\min}}^{M_\perp^{W,\max}} dM \frac{d\sigma}{dM_\perp^W}(M), \qquad (5)$$

with $M_\perp^{W,\min} = 50$ GeV and $M_\perp^{W,\min} = 100$ GeV. The motivation to define $\tilde{\mathcal{O}}$ is that in this way normalization effects, irrelevant for the m_W determination, cancel out, and one is left only with the contribution of PDF uncertainties that induce shape distorting effects. The use of normalized distributions has also been adopted in the Tevatron analysis [4].

The same NLO PDFs are used both to generate the Born and NLO-QCD distributions. In Figs. 4 and 5 we compare, for the three PDF sets, the relative size of the pure PDF uncertainties, at the Tevatron and at the LHC 7 and 14 TeV, for the transverse mass distributions computed at Born level with the HORACE generator. In the latter case, we consider separately the two cases of W^+ and W^- production, since in a proton-proton collider the two distributions are different unlike in a proton-antiproton collider. We show both the standard, Eq. (4), and the normalized, Eq. (5), distributions.

We observe that the PDF uncertainties in the normalized distributions are much smaller than in the standard transverse mass distributions: the reason for this is that variations in the normalization of the distribution, which are not relevant for the determination of m_W, cancel out in the normalized distributions. Note that from Figs. 4 and 5 we see that PDF uncertainties are at the few permille level.

The previous plots show that PDF uncertainties are similar for the three global PDF sets. However, it could still be the case that the distributions obtained with the central set of each PDF set differ sizably among them,

[1] As opposed to other relevant LHC processes, like Higgs boson production via gluon fusion, where α_s uncertainties can be the dominant theoretical uncertainty [29].

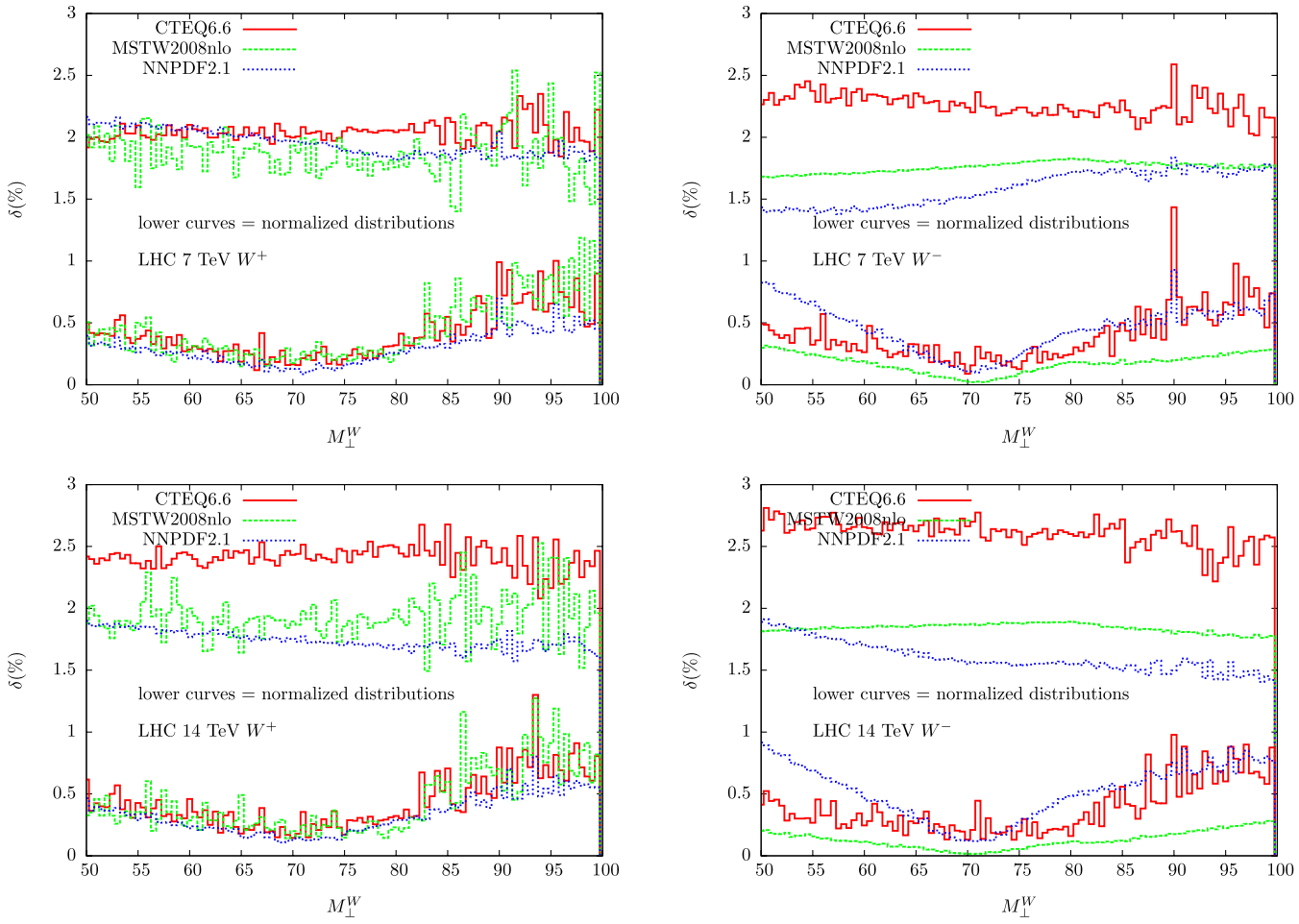

FIG. 4 (color online). Relative PDF uncertainties in the Born level transverse mass distributions, computed with respect the respective central PDF set. From top to bottom: LHC 7 TeV W^+ and W^- and LHC 14 TeV W^+ and W^-. Both the PDF uncertainties on the standard distribution, Eq. (4), and the normalized distribution, Eq. (5), are shown.

leading to an uncertainty in m_W much larger than the nominal PDF uncertainty of a single set. To check that this is not the case, in Figs. 6 (for the LHC) and 7 (for the Tevatron) we show the ratio of transverse mass distributions for each central PDF set normalized to the central CTEQ6.6 predictions.

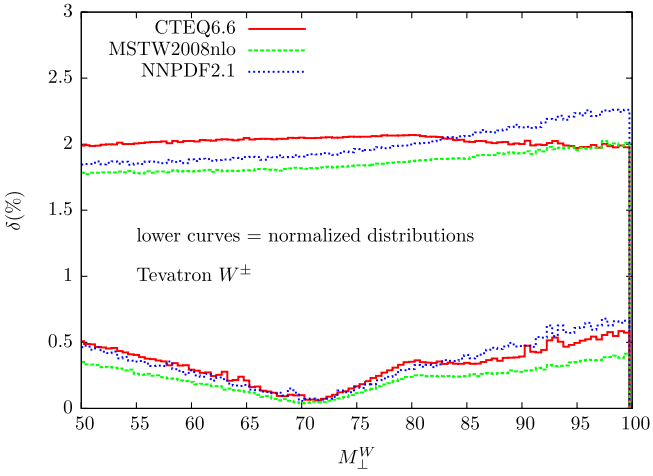

FIG. 5 (color online). Same as Fig. 4 for the Tevatron.

The results of Figs. 6 and 7 show that, while the standard transverse mass distributions differ at the few percent level between different PDF sets, the normalized distributions on the other hand are much more similar, providing an excellent agreement of the central values and differing only at the permille level. This is the same order of magnitude as the intrinsic PDF uncertainties. This suggests that the determinations of m_W from the three different sets are consistent within the respective PDF uncertainties: we will explicitly verify this expectation in Sec. IV.

The uncertainties on the transverse mass distributions, this time computed with the DYNNLO generator at NLO-QCD, are shown in Figs. 8 and 9. The QCD corrections introduce a new partonic subprocess ($qg \to ql\nu_l$) and the related gluon density uncertainty. The latter induces an increase of PDF uncertainties in the large tail of the transverse mass distribution above the Jacobian peak, where the cross section steeply falls, as well as for small

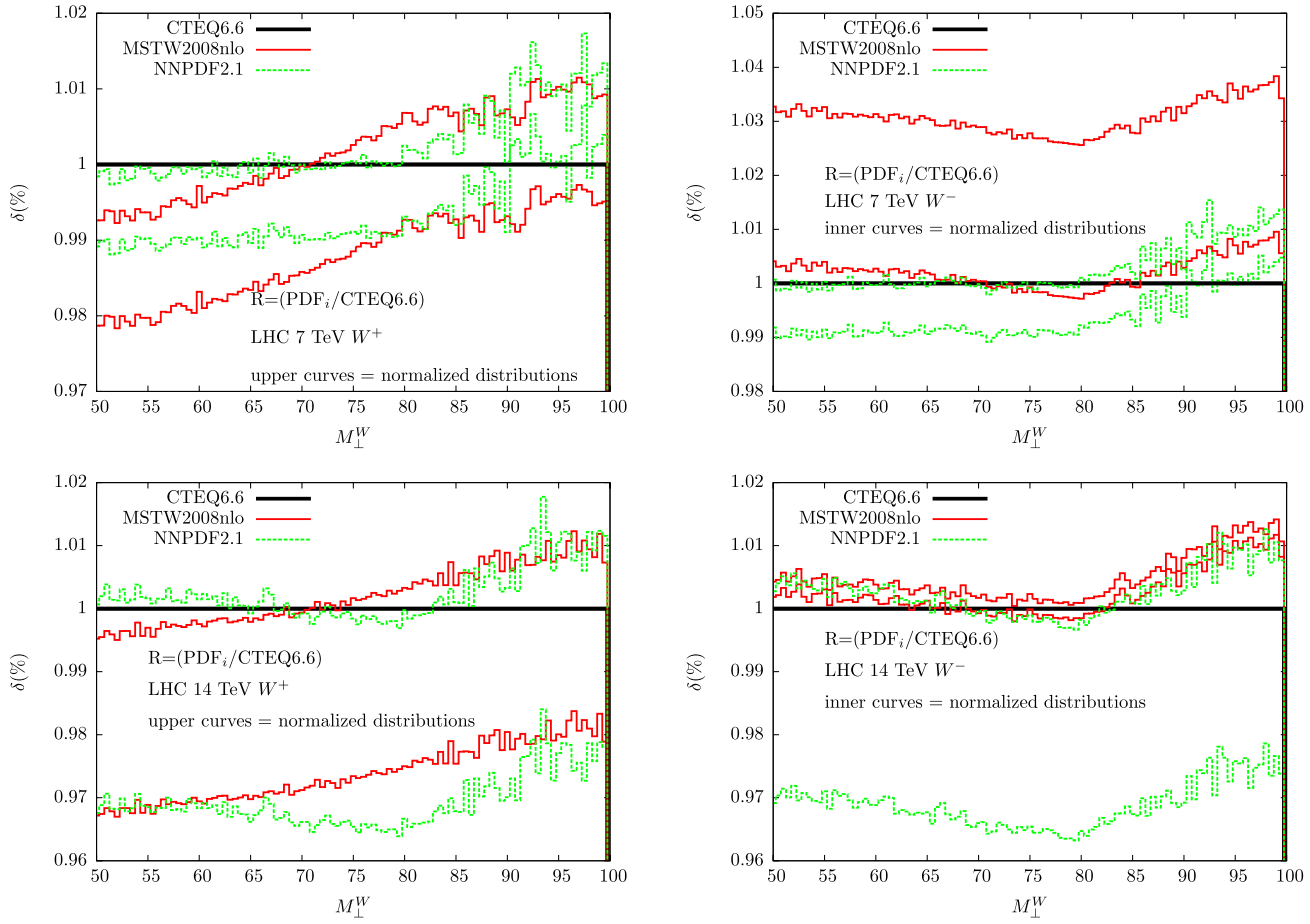

FIG. 6 (color online). Relative difference between the distributions obtained with the central PDF set of CTEQ6.6, MSTW08 and NNPDF2.1, normalized to the CTEQ6.6 result. We show the results both for the normalized and for the standard distributions for LHC 7 TeV (upper plots) and 14 TeV (lower plots).

transverse masses. On the other hand, in the region near the peak, most relevant for the determination of m_W, the PDF uncertainties at NLO-QCD are similar to those of the Born distributions.

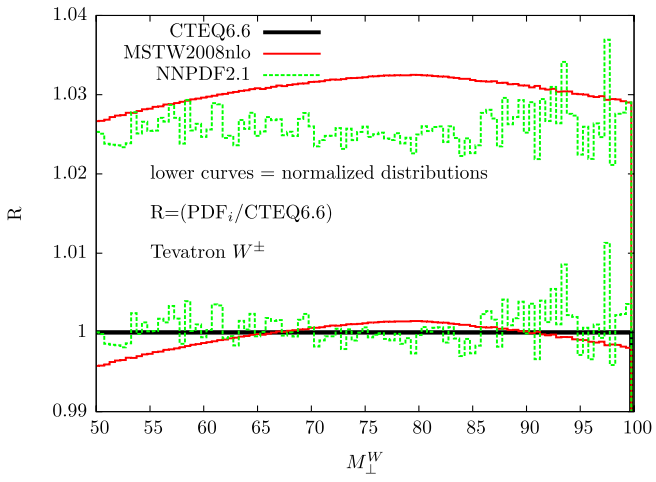

FIG. 7 (color online). Same as Fig. 6 for the Tevatron.

In the transverse mass distributions normalized to their respective cross sections, the difference in PDF normalization has been removed and the uncertainty is due only to the different shapes induced by the PDF sets considered. The comparison in Figs. 8 and 9 shows that the typical size of the PDF uncertainty on these normalized observables is well below the 1% level, whereas in the non-normalized case it ranges between 2 and 3%. The latter are the typical PDF uncertainties that one finds for the inclusive cross section [22].

In Fig. 10 we show, in the case of the NNPDF2.1 set, how the PDF uncertainties in the NLO-QCD transverse mass distribution varies with the energy, collider type and final state. The different uncertainties are very similar in size (e.g., they are all at 2% level, below 80 GeV). Figure 10 shows that PDF uncertainties in the transverse mass distribution are relatively independent of the collider and final state. This result is reassuring since it shows that, at least from the PDF point of view, the determination of m_W at the LHC is not more challenging than at the Tevatron.

Let us now assess the impact of the uncertainties related to the values of α_s and m_c on the transverse mass

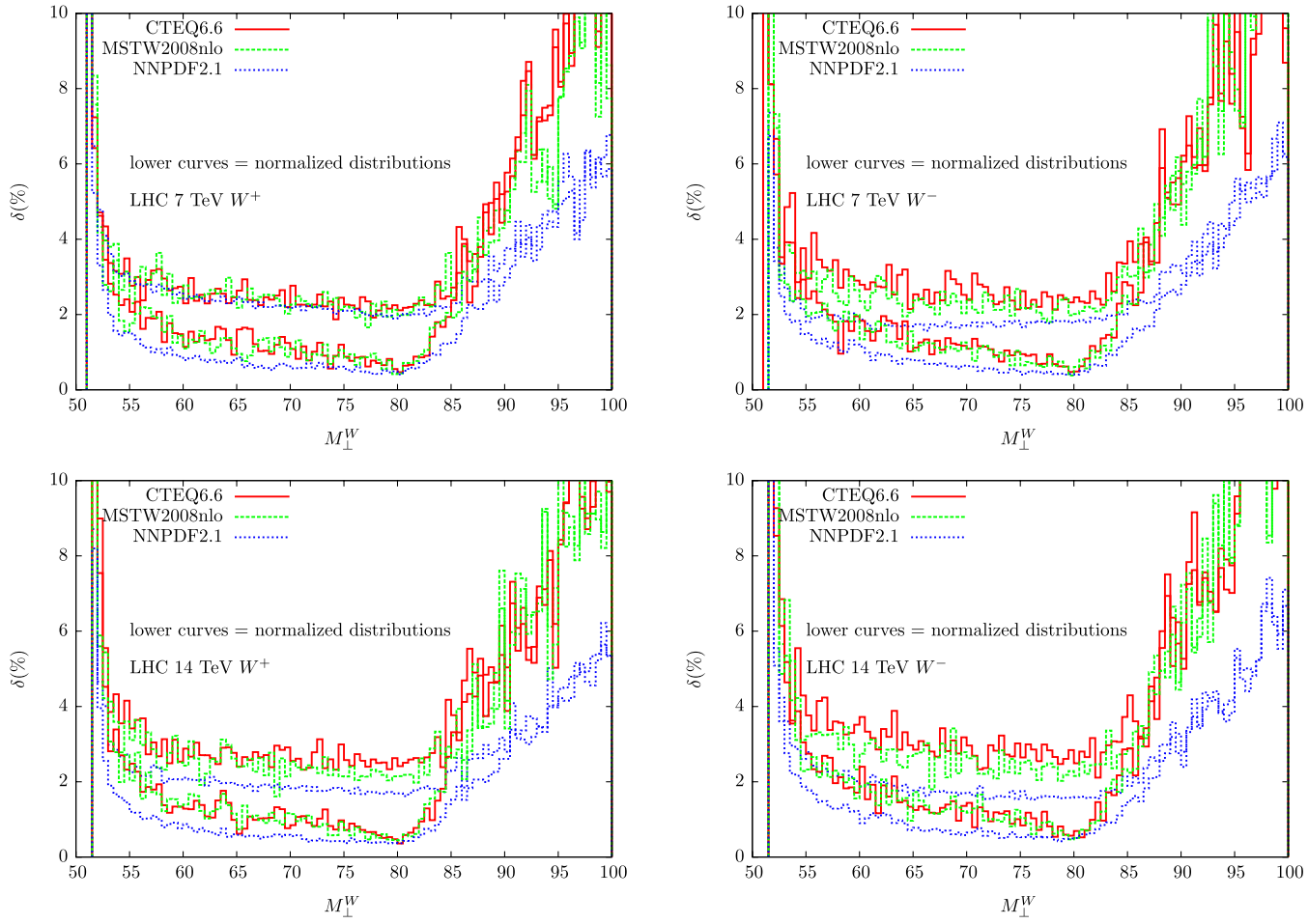

FIG. 8 (color online). Same as Fig. 4 but now the transverse mass distributions have been computed at NLO-QCD using the event generator DYNNLO.

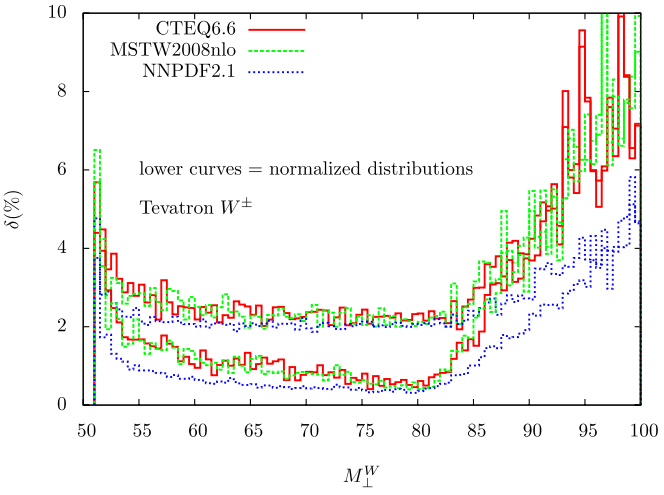

FIG. 9 (color online). Same as Fig. 5 but now the transverse mass distributions have been computed at NLO-QCD using the event generator DYNNLO.

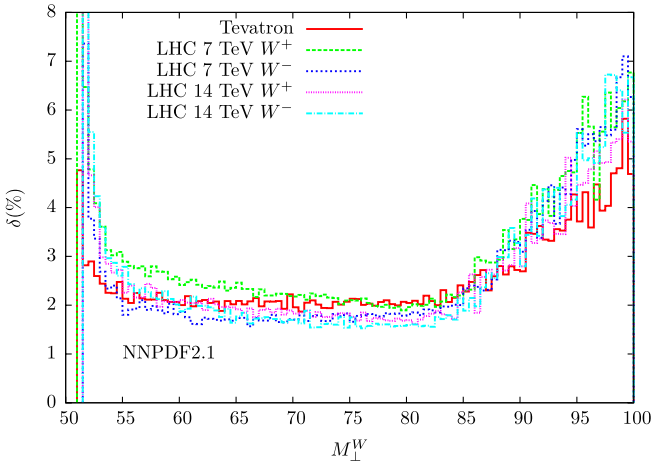

FIG. 10 (color online). The relative PDF uncertainty in the standard transverse mass distributions for NNPDF2.1 for different colliders, energy, and final states.

distribution. In Fig. 11, we show for NNPDF2.1 the PDF–only uncertainty compared to the combined PDF + α_s uncertainty. Following Ref. [27], we assume that the uncertainty on the strong coupling is $\delta_{\alpha_s} = 0.0012$ at the 68% confidence level. For simplicity, we show only the distributions at the LHC 7 TeV: the distributions for Tevatron and LHC 14 TeV are quantitatively very similar. We conclude that α_s uncertainties are negligible as compared to the PDF uncertainties for this distribution.

We have also studied the dependence of the results on the value of m_c used in the PDF determination (using the NNPDF2.1 set with m_c variations), taking fully into account all correlations between m_c and the PDFs. In Fig. 12, we show the ratio of transverse mass distributions computed with different m_c in the PDFs, divided by the results of the central NNPDF2.1 set. It is clear from these results that a different choice of the charm mass in the evolution of the parton densities yields a different overall normalization of the transverse mass distribution, but it affects very moderately the shape. This is confirmed by the normalized distributions: the percentage difference with respect to the reference m_c value is consistent with zero within statistical fluctuations.

In summary, we found in this section that PDF uncertainties in the transverse mass distribution can be kept at the permille level by normalizing them to the integrated cross section in the fitted interval. These PDF uncertainties turn out to be very similar for all colliders, energies and final states, and are in reasonable agreement between different PDF sets. The theoretical uncertainties related to m_c and α_s, that are important for inclusive cross sections, turn out to be negligible for the normalized kinematical distributions. In the next section, we will assess the impact of these various uncertainties on the determination of m_W.

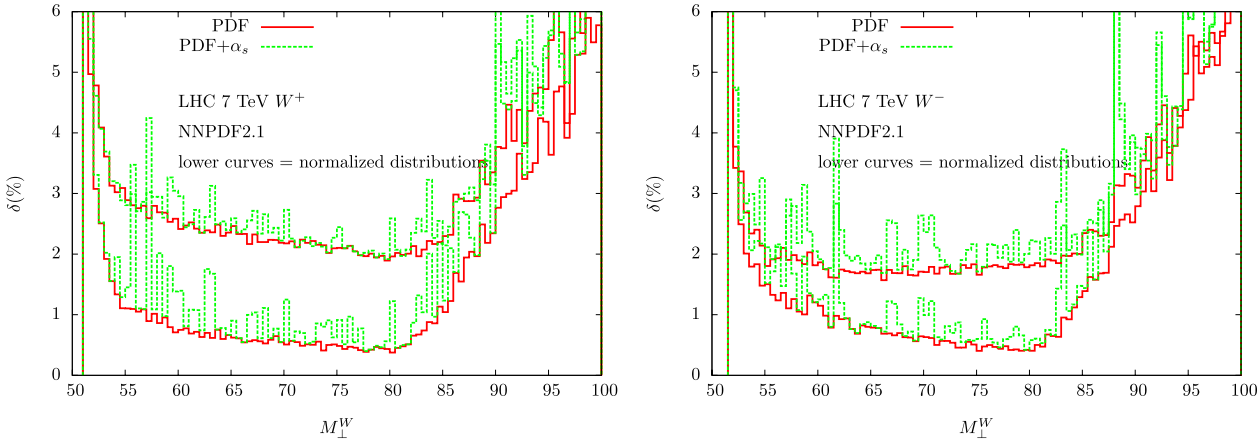

FIG. 11 (color online). Comparison of the PDF–only uncertainty and the combined PDF + α_s uncertainty of the transverse mass distribution for NNPDF2.1. For simplicity we show only the distributions at the LHC 7 TeV, the distributions for Tevatron and LHC 14 TeV are quantitatively very similar.

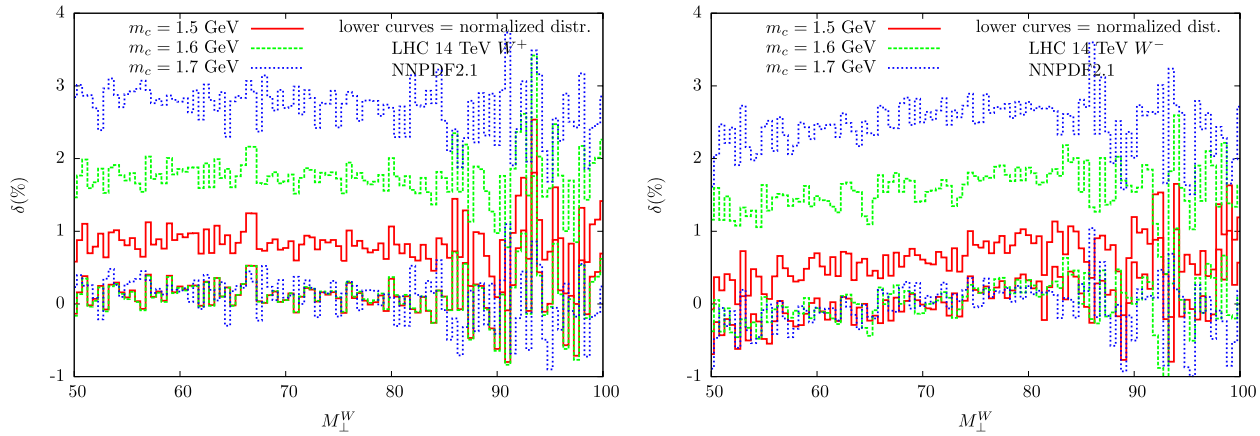

FIG. 12 (color online). For NNPDF2.1 we show the dependence on m_c of the transverse mass distribution, expressed as relative deviation from the central NNPDF2.1 set with $m_c^2 = 2$ GeV^2. We show results both for the normalized and for the standard transverse mass distributions. We consider only the LHC 14 TeV case, where charm mass effects are known to be more important.

TABLE III. Results for the determination of m_W from normalized transverse mass Born distributions. We show in each case the central value of the fit of m_W and the spread due to PDF uncertainties, $\delta_{\rm pdf}$ in GeV. We also indicate well as $\Delta_{\rm pdf}$ (in MeV), the shift in central predictions from each set compared to the CTEQ6.6 reference.

collider, final state	CTEQ6.6		MSTW2008		NNPDF2.1	
	$m_W \pm \delta_{\rm pdf}$	$\Delta_{\rm pdf}$	$m_W \pm \delta_{\rm pdf}$	$\Delta_{\rm pdf}$	$m_W \pm \delta_{\rm pdf}$	$\Delta_{\rm pdf}$
Tevatron, $W^{\pm}$	80.398 ± 0.004	0	80.399 ± 0.003	+1	80.399 ± 0.005	+1
LHC 7 TeV W^+	80.398 ± 0.003	0	80.404 ± 0.003	+6	80.401 ± 0.003	+3
LHC 7 TeV W^-	80.398 ± 0.002	0	80.396 ± 0.002	−2	80.400 ± 0.004	+2
LHC 14 TeV W^+	80.398 ± 0.003	0	80.402 ± 0.002	+4	80.399 ± 0.003	−1
LHC 14 TeV W^-	80.398 ± 0.002	0	80.398 ± 0.002	0	80.398 ± 0.005	0

TABLE IV. Same as Table III for m_W fits to the standard transverse mass distributions.

collider, final state	CTEQ6.6		MSTW2008		NNPDF2.1	
	$m_W \pm \delta_{\rm pdf}$	$\Delta_{\rm pdf}$	$m_W \pm \delta_{\rm pdf}$	$\Delta_{\rm pdf}$	$m_W \pm \delta_{\rm pdf}$	$\Delta_{\rm pdf}$
Tevatron, $W^{\pm}$	80.398 ± 0.007	0	80.408 ± 0.007	+10	80.407 ± 0.008	+9
LHC 7 TeV W^+	80.398 ± 0.007	0	80.399 ± 0.006	+1	80.398 ± 0.005	0
LHC 7 TeV W^-	80.398 ± 0.004	0	80.401 ± 0.004	+3	80.399 ± 0.005	+1
LHC 14 TeV W^+	80.398 ± 0.008	0	80.393 ± 0.007	−5	80.388 ± 0.005	−10
LHC 14 TeV W^-	80.398 ± 0.005	0	80.399 ± 0.004	+1	80.391 ± 0.005	−7

IV. PDF UNCERTAINTIES IN THE DETERMINATION OF m_W

We have shown in the previous section how PDF uncertainties distort the shape of the transverse mass distribution. Now we use the fit setup presented in Sec. II to extract for each template the associated value of m_W, and check how the values of m_W obtained with different PDF sets compare to each other and with their intrinsic PDF uncertainties. We fit the W mass separately with each different Monte Carlo replica (for NNPDF2.1) or with the various Hessian eigenvectors (for MSTW2008 and CTEQ6.6), and then apply the corresponding prescriptions to compute the best estimate for m_W and the associated PDF uncertainty for each set.

In Table III, we present the results obtained when fitting the Born level normalized transverse mass distributions (Eq. (5)). Then in Table IV, we show the analogous results obtained when fitting the standard distributions (Eq. (4)). In both cases, we quote the intrinsic PDF error from each set, denoted by $\delta_{\rm pdf}$ (in GeV), as well as the shift between each set and the reference value obtained with CTEQ6.6, denoted by $\Delta_{\rm pdf}$ (in MeV).

We note that the values of m_W obtained with the standard distributions are shown here only for illustration of the sensitivity of the template fit procedure to the normalization choice. The templates have been prepared at Born level, separately for each energy, collider type and final state. In this way we can claim that in each case we are probing only the effect due to the PDF uncertainty. We remark that the central value of CTEQ6.6 coincides, by construction, with the value ($m_W^0 = 80.398$ GeV) used when generating the pseudodata.

TABLE V. Results for the determination of m_W from normalized transverse mass NLO-QCD distributions. We show in each case the central value of the fit of m_W and the spread due to PDF uncertainties, $\delta_{\rm pdf}$ in GeV. In the right column of each PDF set, the average $\langle \chi^2 \rangle$ per degree of freedom obtained in the fit of the PDF error sets is shown, as a measure of the fit quality. For each collider and final state, the final column estimates the total PDF uncertainty $\delta_{\rm pdf}^{\rm tot}$ using the envelope method, as discussed in the text. A graphical representation of the results is shown in Fig. 13.

	CTEQ6.6		MSTW2008		NNPDF2.1		
	$m_W \pm \delta_{\rm pdf}$	$\langle \chi^2 \rangle$	$m_W \pm \delta_{\rm pdf}$	$\langle \chi^2 \rangle$	$m_W \pm \delta_{\rm pdf}$	$\langle \chi^2 \rangle$	$\delta_{\rm pdf}^{\rm tot}$
Tevatron, $W^{\pm}$	80.398 ± 0.004	1.42	80.398 ± 0.003	1.42	80.398 ± 0.003	1.30	4
LHC 7 TeV W^+	80.398 ± 0.004	1.22	80.404 ± 0.005	1.55	80.402 ± 0.003	1.35	8
LHC 7 TeV W^-	80.398 ± 0.004	1.22	80.400 ± 0.004	1.19	80.402 ± 0.004	1.78	6
LHC 14 TeV W^+	80.398 ± 0.003	1.34	80.402 ± 0.004	1.48	80.400 ± 0.003	1.41	6
LHC 14 TeV W^-	80.398 ± 0.004	1.44	80.404 ± 0.006	1.38	80.402 ± 0.004	1.57	8

Let us consider first the results obtained with normalized distributions, shown in Table III. The central values obtained with MSTW2008 and with NNPDF2.1 (that is the spread of $\Delta_{\rm pdf}$ values) differ at most by 6 MeV with respect to m_W^0 and lie in general in a $\Delta_{\rm pdf} \sim 2$–4 MeV interval. The PDF uncertainties are stable when considering different colliders, energies and final states. If we now look at the results obtained with the standard distributions, Table IV, we observe that the central values are spread in a larger interval (± 10 MeV) and that also the PDF uncertainties are correspondingly increased, $\delta_{\rm pdf} \sim 5$–8 MeV. However, it is remarkable that even for the standard transverse mass distributions PDF uncertainties turn out to be rather small and similar for all colliders and final states.

In Table V, we present the results obtained by fitting the transverse mass distribution generated at NLO-QCD with DYNNLO, with different PDF sets. The main difference with respect to the study at Born level comes from the gluon contribution, absent in lowest order. We fit the distributions, normalized to their cross section in the fitting interval, using DYNNLO templates prepared with the central CTEQ6.6 set and normalized. In Table V, we also provide the average $\langle \chi^2 \rangle$ obtained from the fit to the error PDFs in each case. These results are represented graphically in Fig. 13.

The estimate of the PDF uncertainties for m_W is quite stable at different energies and colliders. The values obtained here are moderately larger than at Born level. To estimate the total PDF error, following the PDF4LHC recommendation, we take the envelope of the results from the three different PDFs sets. This total PDF error obtained with the envelope method, denoted by $\delta_{\rm pdf}^{\rm tot}$ in Table V, is always smaller than 10 MeV (see also Fig. 13). Note, in particular, the excellent agreement of the results from the three sets at the Tevatron, both in central value and in PDF uncertainty, yielding a total PDF uncertainty of only $\delta_{\rm pdf}^{\rm tot} = 4$ MeV.

The above estimates of the PDF uncertainties are somewhat smaller than previous estimates: for example, Ref. [10] estimates $\delta_{\rm pdf}^{\rm tot} \sim 25$ MeV prior to LHC data.[2] We would like to emphasize that the key in reducing the PDF uncertainties is fitting to the normalized kinematic distributions, in a way that normalization effects in PDF uncertainties, irrelevant for the m_W, cancel out. To illustrate this point, we note that from the results for m_W obtained from the Born standard distributions, Table IV, and using the envelope of the three PDF sets, one finds $\delta_{\rm pdf}^{\rm tot} = 12$ MeV at Tevatron, $\delta_{\rm pdf}^{\rm tot} = 7(6)$ MeV at $W^+(W^-)$ LHC 7 TeV and $\delta_{\rm pdf}^{\rm tot} = 12(9)$ MeV at $W^+(W^-)$ LHC 14 TeV, larger than the results of Table III (5 MeV, 6 MeV, 5 MeV, 5 MeV and 4 MeV, respectively) and closer to previous estimates. Our estimates for PDF uncertainties on m_W at the Tevatron are also smaller than existing CDF and D0 estimates [4]. There is work in progress trying to understand these various results and the differences and similarities of the approaches.

[2]This uncertainty, computed from CTEQ6L, is to be understood as a 90% C.L. and thus $\delta_{\rm pdf}^{\rm tot} \sim 15$ MeV at 68% C.L.

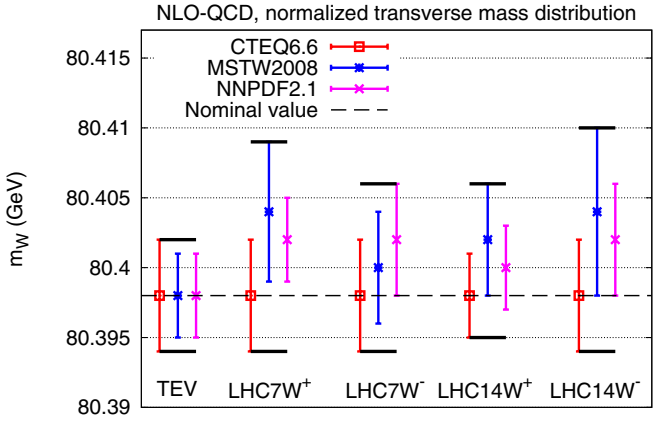

FIG. 13 (color online). Graphical representation of the results of Table V for the various colliders and final states considered. In each case we draw the envelope of the results from the PDF sets to define the total PDF uncertainty ($\pm\, \delta_{\rm pdf}^{\rm tot}$) as a thick solid line. The dashed line marks the position of the nominal value $m_W^0 = 80.398$ GeV used to generate the pseudodata.

In Table VI we present the results obtained by fitting the normalized transverse mass distributions, at the Tevatron, with RESBOS and with CTEQ6.6. The templates used in the fit have been computed with RESBOS as well, with the central CTEQ6.6 set. Note that within the public version of RESBOS, only the CTEQ6.6 set can be used. By construction, the central values of the fit coincide with the nominal input value m_W^0. The results for the PDF uncertainties are similar to those obtained with DYNNLO at NLO-QCD.

Let us consider now the impact of the values of m_c and α_s on the determination of m_W, which we know to be small from the analysis of the transverse mass distributions. In Table VII, we show the results found in the determination of m_W for the case of the NNPDF2.1 fits with varying strong coupling. As expected from the distributions of Fig. 11, differences are negligible, confirming that the uncertainty

TABLE VI. Results for the determination of m_W from normalized transverse mass NLO + NLL QCD distributions generated with RESBOS. We show the central value of the fit of m_W and the spread due to PDF uncertainties, $\delta_{\rm pdf}$ in GeV for the case of the Tevatron. The distributions, normalized to the corresponding cross section in the fitting interval, have been computed using RESBOS and have been fit with templates prepared as well with RESBOS (with the central set of CTEQ6.6).

collider, final state	CTEQ6.6 $m_W \pm \delta_{\rm pdf}$
Tevatron, $W^\pm$	80.398 ± 0.006

TABLE VII. Central value of the fit of m_W obtained with NNPDF2.1, using PDF sets that differ by the $\alpha_s(m_Z)$ value, for different colliders and energies. The fit has been done on normalized distributions and using normalized templates, and the distributions have been generated at NLO-QCD with DYNNLO.

	Tevatron	LHC7W+	LHC7W−	LHC14W+	LHC14W−
$\alpha_s(m_Z) = 0.118$	80.398	80.400	80.398	80.402	80.400
$\alpha_s(m_Z) = 0.119$ (ref)	80.398	80.402	80.402	80.400	80.402
$\alpha_s(m_Z) = 0.120$	80.398	80.400	80.398	80.402	80.402

TABLE VIII. Central value of the fit of m_W obtained with NNPDF2.1 sets with different values of m_c for different colliders and energies. We include the default value in NNPDF2.1, $m_c^2 = 2$ GeV^2 as well.

m_W (GeV)	Tevatron	LHC7W+	LHC7W−	LHC14W+	LHC14W−
$m_c = 1.414$ (ref)	80.398	80.402	80.402	80.400	80.402
$m_c = 1.5$	80.398	80.400	80.398	80.398	80.399
$m_c = 1.6$	80.398	80.400	80.400	80.398	80.399
$m_c = 1.7$	80.396	80.400	80.400	80.396	80.398

in α_s does not play a role for the determination of m_W at hadronic colliders.

In Table VIII, we show the results obtained by fitting the Born level transverse mass distributions generated with the NNPDF2.1 sets extracted with different values of m_c. As is evident from Fig. 12, the results differ mainly in their normalization. Indeed, we observe that the results of the Born level fit of the normalized distributions have very small deviations with respect to the reference value for the charm mass, at most 4 MeV. This is to be compared with the sizeable shifts, at the percent level, observed in the inclusive cross sections when m_c is varied in the global fit. Again, the origin of these different behaviors is that while cross sections depend on the normalization of the distribution and thus of the PDFs, m_W depends only on its shape.

V. THE IMPACT OF LHC DATA ON THE m_W MEASUREMENT

In the previous sections we have discussed the impact of PDF uncertainties on the determination of m_W at hadron colliders. The PDF sets considered there summarize our understanding of the proton structure prior to the LHC. However, LHC data is already providing stringent constraints on available PDF, and thus it will further reduce the effects of PDF errors in the extracted value for m_W. As an illustration of this point, in this section we explore the impact that recent ATLAS and CMS measurements of the lepton asymmetry from W decays have on the determination of m_W.

The CMS and ATLAS experiments have recently presented their measurements of the lepton charge asymmetry from W bosons at 7 TeV. The ATLAS analysis [35] corresponds to muon asymmetries while the CMS analysis [36] contains both the electron and the muon asymmetries for two cuts of the lepton transverse momentum, $p_T \geq 25$ GeV and $p_T \geq 30$ GeV. We have determined the impact of these LHC measurements on the NNPDF2.1 set by means of the Bayesian reweighting technique of Ref. [37]. Preliminary results were presented in [38], and a more detailed analysis will be presented elsewhere. For the comparison with LHC data, the theoretical predictions were generated at NLO with the DYNNLO event generator with the same binning and cuts as in the respective experimental analysis.

We consider two cases: one in which the NNPDF2.1 set includes the impact of the published CMS and ATLAS lepton asymmetry data and another in which the NNPDF2.1 set includes the impact of hypothetical future measurements of the same asymmetries with a relative accuracy of 1% (the average error of the published data is about 7%).

We show the m_W distributions obtained with the $N_{\rm rep} = 100$ replicas of NNPDF2.1 at the LHC 7 TeV and the same NNPDF2.1 replicas reweighted with the lepton asymmetry data in Fig. 14 (left plot). The spread of the distribution indicates the PDF uncertainty in the determination of m_W. We can see that present data already act in the direction of narrowing the distribution thus reducing the PDF uncertainties in m_W, although the constraints are still moderate.

Larger effects are expected in the scenario with lepton asymmetry pseudodata with a 1% bin-per-bin total experimental uncertainty. We can see that these very accurate pseudodata have the potential to narrow the m_W distribution and thus to reduce the PDF error on m_W by a factor of 2 or even more. PDF uncertainties could be further decreased if additional observables, sensitive to the quark and antiquark combinations relevant for m_W production, were considered. One example is provided by the accurate

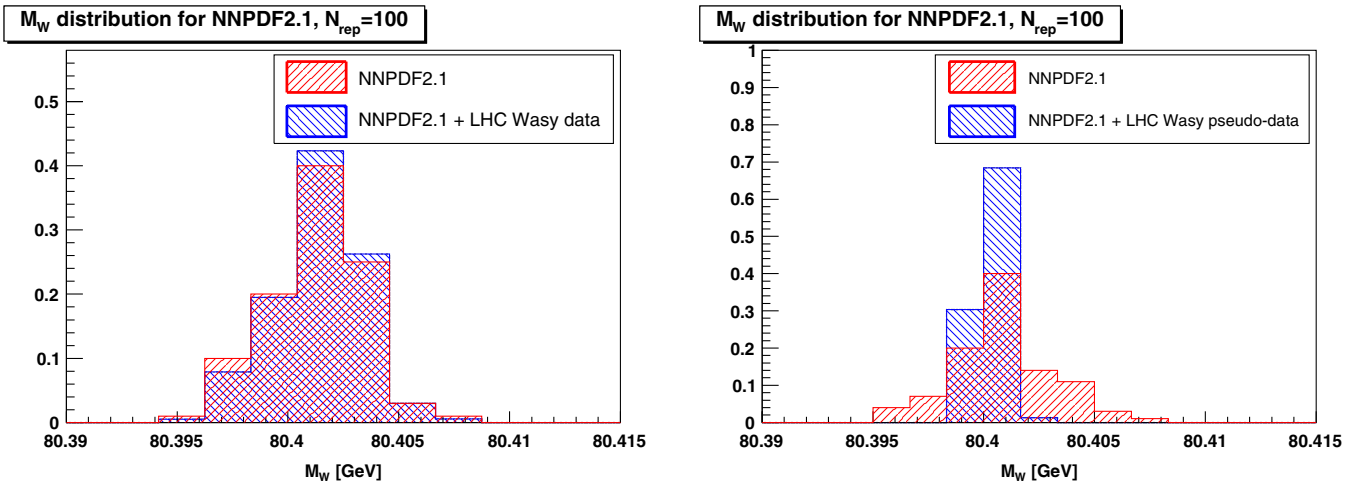

FIG. 14 (color online). The distribution of the 100 values of m_W obtained from each of the 100 replicas of the NNPDF2.1 analysis at the LHC 7 TeV, compared to the results of reweighting NNPDF2.1 with the recent ATLAS and CMS data on W lepton asymmetries (left plot) and by the reweighting of W lepton asymmetries pseudodata at the same kinematics than the published LHC data but assuming with a 1% total experimental uncertainty (right plot). In each case, the spread of the distributions represents the PDF uncertainty. See text for more details.

measurement of the Z boson rapidity distribution at the LHC, that would constrain the small-x sea quarks.

This exercise confirms that, though PDF uncertainties in the determination of m_W are already small, they can be further decreased systematically by LHC measurements.

VI. CONCLUSIONS

In this paper, we have presented a detailed study of the impact of PDF uncertainties on the accurate determination of the W boson mass in hadronic collisions. We have concentrated on the shape of the transverse mass distribution and we have used a template fit technique to determine a preferred m_W value, isolating the PDF effects from other sources of theoretical uncertainties.

Our main conclusions are the following:

(i) The Born level study shows that the prediction of the central values and of the PDF uncertainties agree between the different PDF sets and are stable when comparing different colliders, energies and final states.

(ii) The NLO-QCD study shows results analogous to the Born level case, with a moderate increase of the PDF uncertainty induced by the gluon initiated subprocesses.

(iii) The use of accurate templates, prepared for each specific collider, energy and final state, allows to disentangle the role of the PDFs, while keeping fixed all the other input parameters.

(iv) A sensible and more accurate fit of the W mass can be obtained by studying the shape of kinematical distributions, removing normalization effects which should not be explained in terms of m_W shifts.

(v) PDFs and related uncertainties (α_s, m_c) are estimated to be smaller than 10 MeV at the LHC for all energies and final states, even before accounting for the improvements from LHC data. This implies that PDF uncertainties will be smaller than other systematic uncertainties.

(vi) PDF uncertainties, that are already rather moderate, can be further reduced using LHC data alone, without the need of a new dedicated experimental program to constrain PDFs. We have illustrated this point using the recent lepton asymmetry data from CMS and ATLAS. Measurements of the Z rapidity distribution and other observables will soon further reduce PDF uncertainties. Therefore, a measurement at the level of 10 MeV precision at the LHC, while challenging from many other points of view, does not seem to be forbidden by the uncertainties in our knowledge of the proton structure.

The precision determination of m_W is one of the goals of the current 7 TeV run at the LHC, due to its potential to indirectly probe new physics at the electroweak scale. This study ensures that an accuracy of 10 MeV is certainly within reach, at least in what concerns our present knowledge of the structure of the proton.

ACKNOWLEDGMENTS

We are grateful to M. Mangano for encouragement in this project. We thank C. Carloni Calame, S. Forte, A. Kotwal, G. Montagna, O. Nicrosini, and O. Stelzer-Chilton for stimulating discussions. We are grateful to M. Ubiali for providing the DYNNLO predictions with NNPDF2.1 for the ATLAS and CMS lepton asymmetry data discussed in Sec. V.

[1] http://lepewwg.web.cern.ch/LEPEWWG/.

[2] A. Hoecker (Gfitter Collaboration), Proc. Sci., EPS-HEP2009 (2009) 366.

[3] S. Heinemeyer, W. Hollik, A. M. Weber, and G. Weiglein, J. High Energy Phys. 04 (2008) 039.

[4] Tevatron Electroweak Working Group, CDF Collaboration, and D0 Collab, arXiv:0908.1374.

[5] V. M. Abazov *et al.* (D0 Collaboration), Phys. Rev. Lett. **103**, 141801 (2009).

[6] T. Aaltonen *et al.* (CDF Collaboration), Phys. Rev. D **77**, 112001 (2008).

[7] T. Aaltonen *et al.* (CDF Collaboration), Phys. Rev. Lett. **99**, 151801 (2007).

[8] J. Zhu (CDF Collaboration and D0 Collaboration), AIP Conf. Proc. **1182**, 152 (2009).

[9] V. Büge, Ch. Jung, G. Quast, A. Ghezzi, M. Malberti, and T. Tabarelli de Fatis, Prospects for the precision measurement of the *W* mass with the CMS detector at the LHC, CMS AN 20006/033.

[10] N. Besson, M. Boonekamp, E. Klinkby, T. Petersen, and S. Mehlhase, for (ATLAS Collaboration), Eur. Phys. J. C **57**, 627 (2008).

[11] C. Anastasiou, L. J. Dixon, K. Melnikov, and F. Petriello, Phys. Rev. D **69**, 094008 (2004).

[12] S. Catani, L. Cieri, G. Ferrera, D. de Florian, and M. Grazzini, Phys. Rev. Lett. **103**, 082001 (2009).

[13] G. Balossini *et al.*, J. High Energy Phys. 01 (2010) 013.

[14] M. W. Krasny, F. Dydak, F. Fayette, W. Placzek, and A. Siodmok, Eur. Phys. J. C **69**, 379 (2010).

[15] C. M. Carloni Calame, G. Montagna, O. Nicrosini, and M. Treccani, Phys. Rev. D **69**, 037301 (2004).

[16] C. M. Carloni Calame, G. Montagna, O. Nicrosini, and M. Treccani, J. High Energy Phys. 05 (2005) 019.

[17] C. M. Carloni Calame, G. Montagna, O. Nicrosini *et al.*, J. High Energy Phys. 12 (2006) 016; 10 (2007) 109.

[18] S. Catani and M. Grazzini, Phys. Rev. Lett. **98** 222002 (2007); S. Catani, L. Cieri, G. Ferrera, D. de Florian, and M. Grazzini, *ibid.* **103**, 082001 (2009).

[19] G. A. Ladinsky and C. P. Yuan, Phys. Rev. D **50**, R4239 (1994); C. Balazs, J. w. Qiu, and C. P. Yuan, Phys. Lett. B **355**, 548 (1995)]; C. Balazs and C. P. Yuan, Phys. Rev. Lett. **79**, 2398 (1997); C. Balazs and C. P. Yuan, Phys. Rev. D **56**, 5558 (1997).

[20] P. M. Nadolsky *et al.*, Phys. Rev. D **78**, 013004 (2008).

[21] A. D. Martin, W. J. Stirling, R. S. Thorne, and G. Watt, Eur. Phys. J. C **63**, 189 (2009).

[22] R. D. Ball *et al.* (The NNPDF Collaboration), Nucl. Phys. **B849**, 296 (2011).

[23] S. Forte, Acta Phys. Pol. B **41**, 2859 (2010).

[24] A. De Roeck and R. S. Thorne, arXiv:1103.0555.

[25] S. Alekhin, S. Alioli, R. D. Ball *et al.*, arXiv:1101.0536.

[26] M. Botje *et al.*, arXiv:1101.0538.

[27] S. Dittmaier, C. Mariotti *et al.* (LHC Higgs Cross Section Working Group), arXiv:1101.0593.

[28] https://twiki.cern.ch/twiki/bin/view/LHCPhysics/CrossSectionsCalc, "Practical guide on PDF + α_s error calculation."

[29] F. Demartin, S. Forte, E. Mariani *et al.*, Phys. Rev. D **82**, 014002 (2010).

[30] R. S. Thorne, Phys. Rev. D **73**, 054019 (2006).

[31] S. Forte, E. Laenen, P. Nason, and J. Rojo, Nucl. Phys. **B834**, 116 (2010).

[32] M. A. G. Aivazis, J. C. Collins, F. I. Olness, and W. K. Tung, Phys. Rev. D **50**, 3102 (1994).

[33] J. R. Andersen *et al.* (SM and NLO Multileg Working Group), arXiv:1003.1241.

[34] A. D. Martin, W. J. Stirling, R. S. Thorne, and G. Watt, Eur. Phys. J. C **70**, 51 (2010).

[35] G. Aad *et al.* (ATLAS Collaboration), arXiv:1103.2929.

[36] CMS Collaboration, J. High Energy Phys. 04 (2011) 050.

[37] R. D. Ball *et al.* (The NNPDF Collaboration), Nucl. Phys. **B849**, 112 (2011).

[38] J. Rojo, PDF4LHC meeting, 2011, CERN, http://indico.cern.ch/materialDisplay.py?contribId=4&materialId=slides&confId=127425.